JPET Fast Forward. Published on April 21, 2005 as DOI: 10.1124/jpet.105.084533

Consequences of abrupt glutathione depletion in murine Clara cells: ultrastructural and biochemical investigations into the role of glutathione loss in naphthalene cytotoxicity

Authors: Andrew J. Phimister, Kurt J. Williams, Laura S. Van Winkle, Charles G. Plopper

Departments: Department of Molecular Biosciences (AJP), and Department of Anatomy, Physiology, and Cell Biology (LSVW and CGP), University of California, Davis, School of Veterinary Medicine, Davis, CA 95616; and Department of Pathobiology and Diagnostic Investigation (KJW), Michigan State University, G380 Veterinary Medical Center, East Lansing, MI 48824

Running title: depletion of GSH in Clara cell toxicity

Address all correspondence to: Dr. Andrew J. Phimister, Department of Molecular Biosciences, University of California, Davis, CA 95616

Telephone: (530) 752-5632; Fax: (530) 752-4698; e-mail: aphimister@ucdavis.edu

Text pages: 34

Tables: 1

Figures: 7

References: 37

Words in Abstract: 248

Words in Introduction: 710

Words in Discussion: 1493

Section assignment: Toxicology

Non-standard abbreviations: GSH, reduced glutathione; NA, naphthalene; DEM, diethylmaleate; EtD-1, ethidium homodimer-1

Abstract

Glutathione plays many critical roles within the cell, including offering protection from reactive chemicals. The bioactivated toxicant naphthalene forms chemically reactive intermediates that can deplete glutathione and covalently bind to cellular proteins. Naphthalene selectively injures the non-ciliated epithelial cells of the intrapulmonary airways (i.e. Clara cells). This study attempted to define what role glutathione loss plays in naphthalene cytotoxicity by comparing Swiss-Webster mice treated with naphthalene to those treated with the glutathione depletor diethylmaleate. High-resolution imaging techniques were employed to evaluate acute changes in Clara cell ultrastructure, membrane permeability, and cytoskeleton structure. A single dose of either diethylmaleate (1000 mg/kg) or naphthalene (200 mg/kg) caused similar glutathione losses in intrapulmonary airways (<20% of control). Diethylmaleate did not increase membrane permeability, disrupt mitochondria, or lead to cell death; hallmark features of naphthalene cytotoxicity. However, diethylmaleate treatment did cause Clara cell swelling, plasma membrane blebs, and actin cytoskeleton disruptions similar to naphthalene treatment. Structural changes in mitochondria and Golgi bodies were also noted. Changes in ATP levels were measured as an indication of overall cell function, in isolated airway explants incubated with diethylmaleate, naphthalene, or naphthalene metabolites in vitro. Only the reactive metabolites of naphthalene caused significant ATP losses. Unlike the lethal injury caused by naphthalene, the disruptive cellular changes associated with glutathione loss from diethylmaleate appeared to be reversible, following recovery of glutathione levels. This suggests that glutathione depletion may be responsible for some aspects of naphthalene cytotoxicity, but is not sufficient to cause cell death without further stresses.

Introduction

The epithelium of distal intrapulmonary airways is susceptible to injury from a wide variety of toxicants, including oxidizing gases, aromatic hydrocarbons, and particulate matter. Non-ciliated bronchiolar cells (i.e. Clara cells) are the principal epithelial cell phenotype present in the distal airways of many species, where they are involved in surfactant production, maintaining fluid balance, immune cell regulation, and the metabolism of xenobiotic compounds via cytochrome P450 monooxgenase enzymes (Plopper et al., 1997; Buckpitt et al., 2002). Perhaps the best studied of Clara cell toxicants is the common environmental pollutant naphthalene (NA) (Buckpitt et al., 2002). Exposure to NA selectively results in necrotic lesions in Clara cells regardless of route of exposure (injection, inhalation, ingestion) (Warren et al., 1982; West et al., 2001). This may be because CYP2F2 is the primary cytochrome P450 isozyme responsible for metabolizing NA, and it is highly expressed in Clara cells (Buckpitt et al., 2002). Naphthalene is converted by P450s into highly reactive electrophilic intermediates (e.g. epoxides and quinones) that are primarily detoxified by conjugation to glutathione (GSH). If not detoxified, significant amounts of these reactive metabolites of NA can become attached covalently to proteins (i.e. protein adduct formation) (Warren et al., 1982). Exposure to NA results in a rapid decrease of GSH levels within Clara cells, and a correlation exists between GSH depletion, protein adduct formation, and cytotoxicity (Warren et al., 1982; Plopper et al., 2001; Phimister et al., 2004).

Naphthalene cytotoxicity has been characterized at the ultrastructural level in Clara cells and progresses as follows: endoplasmic reticulum dilation, cytoskeletal disruption, and membrane blebbing, followed by mitochondrial degranulation, plasma membrane leakage, and nuclear condensation (Van Winkle et al., 1999). Studies in hepatocytes have shown a similar progression

of cellular degeneration in response to reactive toxicants (Zahrebelski et al., 1995; Manygoats et al., 2002). GSH loss has been implicated in many of these cellular responses to toxicants (Jewell et al., 1982; Reed and Fariss, 1984; Mirabelli et al., 1988). GSH is involved in vital cellular functions such as antioxidant defense, protein folding, protein synthesis, and intracellular signaling (Uhlig and Wendel, 1992). Severe GSH loss has the potential to disrupt various cellular processes and may be a critical factor in the cytotoxicity of a number of reactive toxicants. We hypothesized that at least a portion of the degenerative cellular changes that characterize NA cytotoxicity in Clara cells (e.g. swelling) occur in response to a radical drop in cellular GSH levels.

In this study, we wanted to determine specifically what effect GSH loss has on Clara cells in the absence of reactive metabolites. To accomplish this goal, we compared Clara cells treated with NA to those given only the GSH depleting agent diethylmaleate (DEM). Diethylmaleate is a weak electrophile and requires active glutathione-S-transferase enzymes in order to deplete GSH (Boyland and Chasseaud, 1967; Plummer et al., 1981). Naphthalene metabolites are conjugated to GSH via glutathione-S-transferase enzymes, however, NA metabolites are reactive enough to spontaneously conjugate with GSH and protein thiol groups in solution (Buckpitt et al., 2002). Therefore, we used DEM in an attempt to study the effects due exclusively to GSH loss in Clara cells, while likely eliminating a confounding factor of NA toxicity, namely protein adduct formation (Fig. 1). It should be noted that we cannot rule out the potential for DEM treatment to have unanticipated side effects on Clara cells through mechanisms unrelated to GSH depletion, (i.e. alkylation of electrophiles), particularly given the high dose of DEM employed (1000 mg/kg). However, DEM had been used in dozens of studies on GSH depletion and appeared to

be a good choice for achieving our goals of rapid and selective GSH depletion. Following treatment of mice with NA or DEM, their airways were examined by high-resolution light, electron, and laser-scanning confocal microscopy to assess changes in Clara cell ultrastructure and membrane permeability, in the context of the previously characterized cellular degeneration caused by NA treatment (Van Winkle et al., 1999). Additionally, we correlated these cellular changes with measurements of GSH levels within distal intrapulmonary airways, which contain predominantly Clara cells (Plopper et al., 1997). This approach allowed us to address the following questions: 1) which features of NA cytotoxicity may be due exclusively to GSH loss, and 2) what effect does abrupt GSH loss have on Clara cells?

Materials and Methods

Chemicals

Naphthalene (NA; +99% purity) and diethylmaleate (DEM; 98.9% purity) were purchased from Aldrich Chemicals (Milwaukee, WI). A racemic mixture of 1,2-naphthalene-oxide was prepared synthetically as described.(Yagi and Jerina, 1975) Mazola corn oil was manufactured by Best Foods/CPC International (Englewood Cliffs, NJ). Aldehyde fixatives were obtained from Electron Microscopy Sciences (Fort Washington, PA). Araldite 502 epoxy resin, osmium tetroxide, lead citrate, and uranyl acetate were obtained from Ted Pella, Inc. (Redding, CA). Ethidium homodimer-1 and Yo-Pro-1 were purchased from Molecular Probes (Eugene, OR). Waymouth's MB 752/1 media, lacking cysteine, cystine, methionine, glutamine, and glutathione was obtained from Gibco (Grand Island, NY). All other chemicals were reagent grade or better.

Animals and Treatment

Male Swiss Webster mice were purchased from Charles River Breeding Laboratories (CFW; Portage, MI). Animals were allowed free access to food and water and were not fasted before treatment. They were housed in HEPA-filtered cage racks on sterile paper fiber bedding for at least 5 days before use in AAALAC approved facilities. For all experiments, animals were given a single intraperitoneal dose of 1000 mg/kg DEM (1 M solution in corn oil), 200 mg/kg NA (234 μM solution in corn oil), or a corresponding volume of corn oil (vehicle control). Solutions were prepared daily. Animals were euthanized with an overdose of pentobarbital sodium.

HPLC Analysis of GSH

Intrapulmonary airways were isolated by microdissection procedures described previously(Plopper et al., 1991) with the modification that the lungs were perfused free of blood with ice-cold 1 mM EDTA/saline. Airway segments were isolated from lungs of mice at 0, 1, 3, 6, and 24 hours after DEM or NA treatment. At least 5 animals were evaluated at each time point for each treatment. A previously described method (Lakritz et al., 1997) was employed for the quantification of GSH. Briefly, acidic tissue homogenates were subjected to reverse-phase HPLC coupled with electrochemical detection to directly measure reduced GSH. The response was linear from 0.5-1000 ng of GSH (R^2 = 0.995) and data are reported as nmol of GSH per mg of homogenate protein, as determined by the Lowry protein assay (Lowry et al., 1951).

High-resolution histopathology and electron microscopy

Lungs were collected from mice treated with DEM, NA or corn oil at 1, 3, 6, and 24 hours after treatment. Three mice were compared for each treatment at each time point. Following exposure, their lungs were inflated *in situ* via a tracheal cannula with dilute Karnovsky's fixative (1% glutaraldehdye/0.5% paraformaldehyde in cacodylate buffer, 330 mOsm, pH 7.4) at 30cm water pressure for 1 hour, followed by overnight storage in the same fixative. After fixation, the left lobes were sliced perpendicular to the long axis of the lobe into 2 mm-thick sections, post-fixed with 1% osmium tetroxide, and embedded in Araldite 502 epoxy resin as described (Van Winkle et al., 1995). One-micron thick sections were stained with 1% toluidine blue. Fields were recorded at 380x magnification on an Olympus BH2 microscope (Olympus International, Melville, NY) with a CoolSNAP cooled CCD-camera (Roper Scientific, Tucson, AZ). Areas of interest were excised from the same blocks of embedded tissue and remounted for ultra-thin sectioning. Ultra-thin sections (70nm) were cut with a Sorvall MT 5000 ultramicrotome (DuPont

Company, Newtown, CT) using diamond knives. Sections were stained with uranyl acetate and lead citrate and examined using a Zeiss EM-10 electron microscope (Zeiss, International) at 80 kV.

Pathology evaluation

To better assess differences in the pathological lesions developing in Clara cells treated with NA or DEM, two types of measurements were employed to help distinguish the extent of these changes. As a measurement of cell swelling in response to toxicant treatment, airway epithelial thickness and cell volume relative to basal lamina surface area V_s ($\mu m^3/\mu m^2$) were determined for DEM treated animals as previously described (Van Winkle et al., 1995); see text of results section. Terminal bronchiolar airways were imaged for each animal (256X magnification) in the same sections used for high-resolution histopathology. Point/intercept counting of vertical sections was performed with a cycloid grid overlay and Stereology Toolbox software (Morphometrix, Davis, CA).

The second type of measurement was to develop a semi-quantitative grading system (criteria listed below). At least five terminal bronchioles were evaluated per mouse, 3 mice per treatment group, using the above criteria. Each mouse was given a score (0-4) and the scores for the mice in each group were averaged, to provide a score indicative of the pathology observed in that group. Means ± SEM are provided for each group in Table 1.

0 similar to untreated control (no vacuoles/even thickness/cuboidal)

1 minimal injury—swollen; some blebs; no vacuoles

2 moderate injury—many blebs; few vacuoled cells; no cells lost

3 moderate/severe injury—many vacuoled cells; some cells lost

4 severe injury—most or all cells vacuolated or lost

Membrane permeability assay

Changes in membrane permeability were examined 6 hours after treatment with DEM, NA, or corn oil by a previously described method (Van Winkle et al., 1999). Briefly, the lungs of these mice were inflated via a tracheal cannula with 5 μM ethidium homodimer-1 (EtD-1) in Ham's F12 media at 37^{o}C. Ethidum homodimer-1 is excluded from cells with intact plasma membranes due to the multiple charges it carries and exhibits a 30-fold increase in fluorescent intensity upon binding to DNA. Following a 10 minute incubation with EtD-1, lungs were washed with fresh F12 media before being fixed with Karnovsky's fixative. The right middle lobe of each animal was microdissected to expose the airway lumen before labeling all nuclei in the tissue with the fluorescent nuclear dye Yo-Pro-1 (4 μM in PBS, pH 7.4). The distribution of permeable airway cells (EtD-1 positive; red fluorescence) within the context of all airway cells (green Yo-Pro-1 fluorescence) was mapped by using a Radiance 2100 laser scanning confocal microscope (Bio-Rad, Hercules, CA), a 10X long working distance water-immersion objective, and the appropriate filter sets (excitation/emission: 488/515 and 543/600). Digital image processing reassembled the individual focal planes to produce a three-dimensional image of the airway detailing the distribution of permeable cells.

Actin Cytoskeleton Imaging

Lungs from mice treated with DEM, NA, or corn oil for 3 or 6 hours were fixed by inflation with 1% paraformaldehyde via a tracheal cannula for at least 1 hour. Following fixation, the right middle lobe was microdissected to expose the airway lumen of terminal bronchioles. The direct-binding F-actin probe, Alexa 568 phalloidin, was used as directed by the manufacturer (Molecular Probes, Eugene, OR). The whole mount preparations were mapped using a Radiance 2100 laser scanning confocal microscope (Bio-Rad, Hercules, CA). Optical sections were taken with the gain, black level, and iris settings optimized on the vehicle-treated controls and then kept unchanged between each treatment. Digital image processing reassembled the individual focal planes into a three-dimensional image of the filamentous actin cytoskeleton at the apical surface of the airway epithelium.

Measurement of ATP Levels

Explants of distal intrapulmonary airways were prepared by microdissection from untreated mice for *in vitro* culture as described (Plopper et al., 1991). Immediately following isolation, isolated airway segments were incubated in 0.5 ml of Waymouth's media in glass vials with Teflon-lined caps at 37^{o}C in a shaking water bath. Stock solutions of DEM, NA, and two NA metabolites were prepared in methanol immediately before addition to the airway explants. Methanol content did not exceed 0.5% of incubation volume. Final concentrations of chemicals were as follows: 0.35 mM DEM, 0.5 mM NA, 0.2 mM NA-oxide, 0.2 mM 2-methyl-1,4-naphthoquinone (Aldrich Chemical Co., Milwaukee, WI). An equivalent volume of methanol was used as a vehicle control. Concentrations of chemicals were selected based on prior studies of the toxicity of NA, NA-oxide, and 1,4-naphthoquinone (Chichester et al., 1994), and GSH depletion in isolated airways (Duan et al., 1996). Airways were incubated with the various compounds for 30 minutes

before being homogenized in 10% perchloric acid. Proteins were separated from supernatant by centrifugation and dissolved in 1N NaOH to assess protein content by the method of Lowry (Lowry et al., 1951) with BSA as a standard. Supernatants were neutralized with 5M K_2CO_3 and assayed for ATP content with a luciferase-based method with an ATP Determination Kit (Molecular Probes, Eugene, OR) according to manufacturer's instructions. At least 5 airways were evaluated for each chemical treatment. Data are expressed as pmol of ATP per mg of airway homogenate protein.

Statistics

All data are reported as the mean ± S.E.M. Significant differences between treatment groups were determined by one-way analysis of variance (ANOVA) and Dunnett's post-hoc testing method at the $P < 0.05$ level.

Results

GSH depletion in airways

Glutathione levels dropped rapidly in response to treatment with DEM or NA (Fig. 2). DEM caused GSH levels to decrease to near 20% of control levels within 1 hour of treatment and by 3 hours to 10% of control levels in bronchiolar airways. NA produced similar decreases in GSH levels. With both treatments, the depletion was transient, with GSH levels rebounding to near control values within 6 hours and rising above steady state levels by 24 hours. The kinetics of GSH loss and the subsequent return to pretreatment GSH levels were qualitatively similar for both NA and DEM treatments. Higher doses of DEM (1.5-2 g/kg) did not increase GSH loss further, while a lower dose (0.5 g/kg) did not bring about sufficient pulmonary GSH losses to effectively model NA treatment (data not shown).

Membrane Permeability and Actin Cytoskeleton Disruption

Laser scanning confocal microscopy was used to generate 3D composite images of permeable cells within the context of the whole airway, from 1 to 24 hours after treatment with DEM, NA or corn oil. The 5 most distal airway generations of the main axial path of the right middle lobe were imaged (Fig. 3A-C). Permeable cells (i.e. necrotic cells) are indicated by red ethidium homodimer-1 labeling presented on a green background of all nuclei within the tissue (Yo-Pro-1 labeling). Previously, we have shown that permeable cells first become apparent 2 hours after administration of NA (200 mg/kg, ip), with maximal numbers of permeable cells being present 6 hours after treatment (Van Winkle et al., 1999). Our current results confirmed this finding, with large numbers of permeable cells being present in terminal airways 6 hours after NA treatment (Fig. 3B, arrows; see inset for close-up of permeable nuclei). In contrast, no increase in

membrane permeability was noted in the airways of mice treated with DEM at any time point up to 24 hours after treatment (Fig. 3C, 6-hour post-DEM treatment shown).

In control animals (corn oil treated), the actin cytoskeleton at the apical surface of the airway epithelium formed tight bundles of cortical actin fibers at junctions between airway epithelial cells (Fig. 3D). These bundles were of regular thickness, and based on their pattern of arrangement, ciliated cells can be distinguished from Clara cells by their angular morphology and presence of actin associated with the terminal web at the cell apex. Exposure to either NA or DEM for 3 hours (Fig. 3E-F) led to alterations in the morphology of Clara cell actin filaments. The cortical actin fibers in both treated groups were irregular and frayed, with occasional actin aggregates noted (asterisks).

High-Resolution Light and Transmission Electron Microscopy

The morphologic appearance of the epithelium in the terminal bronchioles of treated and control mice was compared by light (Fig. 4) and transmission electron microscopy (Fig. 5 and 6). Ciliated cells (CC) were identified by the presence of cilia, while Clara cells (non-ciliated; NC) were identified by their characteristic apical projections (Fig. 4A and 5A). The apical protrusions of Clara cells in control mice (Fig. 5A) contained abundant smooth endoplasmic reticulum (SER), dense secretory granules (G), and mitochondria (M) in both circular and longitudinal profile (Fig. 5B, high magnification image of cell). In control animals, the epithelium was of regular thickness and similar appearance at all time points (3 hour corn oil mouse shown in Fig. 4A and 5A). The general response of Clara cells 1 hour after NA treatment was to swell, with the formation of multiple, small cytoplasmic vacuoles (Fig. 5C). The vacuoles originated within the

SER and appeared to dilate and coalesce into the larger vacuoles and lamellar structures found within the membrane blebs of injured cells 3 hours after NA treatment (Fig. 5D; asterisk). Membrane blebs were separated from cells by thick bands of intermediate filaments (Fig. 5D; area between arrows). Three hours after exposure to NA (Fig. 4B and 5D) the majority of Clara cells in terminal bronchioles were vacuolated (V) and contained membrane blebs (asterisks). These early signs of cellular injury had progressed to frank cell necrosis by 6 hours (Fig. 4C). Twenty-four hours after NA treatment, the epithelium consisted primarily of ciliated cells that had squamated (Fig. 4D; arrows and Fig. 5E "SqCC") to cover the areas of basement membrane vacated by necrotic Clara cells exfoliating (ExNC) into the airway lumen (Fig. 4D and 5E).

Likewise, treatment with DEM caused Clara cells to swell 3 hours after treatment (Fig. 4E and 5F), with cell volume per unit surface area increasing from 5.4 ± 0.9 to 8.1 ± 0.9 $\mu m^3/\mu m^2$ (150% increase; $P < 0.05$). Cell swelling appeared to be decreasing 6 hours after DEM treatment (Fig. 4F) and was not evident by 24 hours (Fig. 4G). Clara cell volume returned to near control values (5.5 ± 0.4 $\mu m^3/\mu m^2$) by 24 hours (Fig. 4A vs. 4G). No statistical increase in ciliated cell volume was noted at any time point after DEM treatment. Drastic increases in Clara cell volume have previously been reported for NA treated mice (Van Winkle et al., 1995). [Note: values for NA induced cell volumes were not included here because the severe blebbing and vacuolization produced by NA, affect cell volume measurements and were not as apparent in DEM treated animals.] Whereas naphthalene treatment caused Clara cells to swell within 1 hour of treatment (Fig. 5C), noticeable swelling was not apparent in Clara cells until 3 hours after DEM was given (Fig. 4E and 5F). Increases in cell volume appeared to be due mainly to dilated SER and small cytoplasmic vacuoles forming within the Clara cells (Fig. 5F). A portion of the Clara cell volume

increase in DEM treated animals was due to large membrane blebs, which extended from the apical cellular surface in about 10% of the terminal bronchiolar Clara cells (Fig. 5G; asterisks). Overall, the amount of SER present seemed to be greatly increased and the major constituent of these membrane blebs. As with Clara cells exposed to NA, the membrane blebs in DEM treated animals were clearly separated from the main cell body by bands of filaments (Fig. 5G; area between arrows). Even in cells lacking membrane blebs, bands of filaments could be seen dividing the cytoplasm, such that the SER was segregated into the apical portions of cells, with mitochondria being packed tightly around the nucleus (not shown). A number of the membrane blebs contained multilamellar bodies (Fig. 5G; arrowheads). The origin of the multilamellar bodies is not known but it appears that they are derived from SER. The individual sheets of the multilamellar bodies resemble individual tubules packed in concentric rings or parallel stacks that are physically associated with SER, and the average width of the individual layers (170 nm) was found to be close to that of SER tubules (250 nm). Gross changes in the appearance of ciliated cells were not observed at any time point in DEM treated animals, however, small membrane blebs were noted in a few of the ciliated cells at 24 hours (Fig. 4G and 5H; asterisks). Interstitial edema was evident in the peribronchiolar region of both NA and DEM treated mice (Fig. 4D and 4H; arrowheads) along with a mild infiltrate of inflammatory cells (not shown). Table 1 provides semi-quantitative data summarizing the pathologic changes noted in the different treatment groups, derived using a scoring system described in the methods section (0 represents no injury and ranges to 4 as maximal injured).

Clara cells from NA and DEM treated animals were evaluated at high magnification (12,500-40,000X) to examine the effects of the treatments on individual organelles. In Clara cells of

control animals, mitochondria (M) in circular profile were surrounded by a double membrane and were filled with electron dense material (Fig. 6A). Clara cells in NA treated animals developed signs of mitochondrial injury, such as swelling and degranulation, first apparent after 3 hours post-NA injection (Fig. 6B) and progressed to full disintegration of affected mitochondria by 6 hours (Fig. 6C). In contrast, DEM treatment did not cause mitochondrial swelling or affect their density (Fig. 6D). However, 24 hours after DEM treatment, a number of mitochondria with branched or dumbbell morphologies were seen (Fig. 6E-F) resembling mitochondria undergoing fission or division (Bereiter-Hahn and Voth, 1994). Clara cells contain prominent Golgi bodies in the basolateral portions of the cell (Fig. 6G). The cisternae of the Golgi bodies were greatly distended 3-6 hours after DEM treatment, with pericanalicular vesicles accumulating on the trans-side of the bodies (Fig. 6H; arrowhead). The distention appeared to resolve 24 hours after DEM treatment as the cisternae regained their normal flattened appearance (Fig. 6I). Golgi bodies could not be easily identified within Clara cells of NA treated animals.

ATP Levels in Terminal Bronchioles Exposed in vitro

The cytotoxicity of DEM, NA, and metabolites of NA to airway epithelium was evaluated by measuring ATP levels in terminal bronchiolar explants isolated by microdissection from untreated mice, as described in the methods section. A drastic drop in ATP levels was taken as general an indication of cytotoxicity. In addition to DEM and NA incubations, bronchioles were incubated with naphthalene-oxide (NA-oxide), the first chemical species formed during the metabolic activation of NA by P450s (CYP2F2) or with 2-methyl-1,4- naphthoquinone (MQ), representative of the naphthoquinones that can be formed during NA metabolism.(Buckpitt et al., 2002) ATP levels were similar in DEM treated bronchioles compared to controls while NA

JPET Fast Forward. Published on April 21, 2005 as DOI: 10.1124/jpet.105.084533
This article has not been copyedited and formatted. The final version may differ from this version.

treatment caused a slight, but not statistically significant, decrease in ATP levels (Fig. 7). Exposure to either of the NA metabolites, NA-oxide or MQ, caused rapid and drastic decreases in bronchiolar ATP levels ($P < 0.05$).

Discussion

In this study, we tested the hypothesis that the progressive cellular degeneration associated with acute cytotoxicity produced by bioactivated pulmonary toxicants occurs in response to a radical drop in cellular GSH levels. We used as a model system the response of Clara cells in mice exposed to naphthalene (NA). Reactive metabolites (e.g. epoxides and quinones) generated during P450 dependent metabolic activation of NA are primarily detoxified through conjugation to GSH and can substantially deplete pulmonary pools of reduced GSH (Buckpitt et al., 1984; Buckpitt et al., 2002). Reactive metabolites can deplete GSH through enzymatic conjugation, direct chemical conjugation, and redox-cycling. They can also form covalent adducts with proteins (Fig. 1), potentially affecting the cell through several pathways (Buckpitt et al., 2002). A correlation appears to exist between GSH loss, protein adduct formation, and NA cytotoxicity (Warren et al., 1982; Plopper et al., 2001; Phimister et al., 2004), but the relative importance of GSH loss has not previously been investigated as a singular event in Clara cell toxicity. Similar correlations between GSH loss and covalent binding to cellular macromolecules have been reported for other bioactivated toxicants (example acetaminophen), and it has led to the hypothesis that reactive metabolites are responsible for cell death by mechanisms that involve covalent interaction with critical cellular macromolecules, with attendant disruption of normal biochemical functions. However, given that GSH plays so many critical roles within the cell (e.g. protein folding, cellular signaling, regulating redox status) (Uhlig and Wendel, 1992; Sies, 1999), and that GSH depletion in the absence of exogenous stressful stimuli can cause cellular injury (Martensson et al., 1991; Chevez-Barrios et al., 2000), we asked whether GSH loss alone was responsible for the cellular degeneration characteristic of NA treatment. We have focused on separating the events associated with GSH loss from those involving protein adduct formation in

naphthalene toxicity through the use of the GSH depleting agent diethylmaleate (DEM) (Ecobichon, 1984; Reed and Fariss, 1984; Gerard-Monnier et al., 1992), to achieve GSH loss in the absence of protein adduct formation. A mildly reactive α,β-unsaturated carbonyl compound, DEM is conjugated to GSH by glutathione S-transferases to form hydrophilic GSH conjugates. Diethylmaleate was chosen for this study because it has been used extensively and has been shown to reduce pulmonary GSH levels very rapidly (Ecobichon, 1984; Reed and Fariss, 1984; Deneke et al., 1985). The commonly used GSH synthesis inhibitor, buthionine sulfoximine (BSO), will lower pulmonary GSH levels, but it has to be administered repeatedly for several days to achieve significant GSH loss in the lung (Martensson et al., 1989). Diethylmaleate treatment effectively modeled NA exposure in terms of GSH loss in distal intrapulmonary airways (Fig. 2). Having a model system in which comparable GSH depletion could be achieved, presumably in the absence chemically reactive species, allowed us to determine which of the degenerative cellular changes previously ascribed to NA cytotoxicity (endoplasmic reticulum dilation, cytoskeletal disruption, membrane blebbing, mitochondrial degranulation, and plasma membrane leakage) (Van Winkle et al., 1999) were due predominantly to GSH loss.

In this study, we demonstrated that cell swelling and membrane bleb formation occur following treatment with either NA or DEM, agreeing with results previously published on the effects of NA treatment on Clara cell ultrastructure (Van Winkle et al., 1999). Both DEM and NA treatment elicit cell swelling and membrane bleb formation, demonstrating a role for GSH loss in the development of these cellular changes. Studies with cells in culture have associated GSH loss with disruptions of the cytoskeleton and membrane bleb formation (Jewell et al., 1982; Reed and Fariss, 1984; Mirabelli et al., 1988). It is believed that blebs are formed primarily because of

cytoskeletal disruptions near the surface of the cell, allowing portions of cytoplasm to become distended. Diethylmaleate has been shown to disrupt actin and tubulin filaments in hepatocytes (Dumont et al., 1991; Nagelkerke et al., 1991), and our results demonstrated that both DEM and NA can alter the actin cytoskeleton (Fig. 3E-F). However, in spite of the similarities between DEM and NA treatment in regards to their effects on cell swelling, blebbing, and actin filament disruption, the outcomes of these two treatments were strikingly different. While DEM treated Clara cells were able to recover from the stresses induced by GSH loss, NA treated cells continued to degenerate past the point of recovery and became necrotic.

One noticeable difference between the two treatments was the mitochondrial swelling and degranulation that resulted from NA exposure, which was absent in DEM treated animals. Mitochondrial damage may be a crucial step in NA-induced cell injury and has been reported previously for NA treated animals (Van Winkle et al., 1995). In studies conducted on isolated hepatocytes, it was shown that cyanide induced hypoxia causes disintegration of the cell only once the mitochondria become disrupted and the mitochondrial membrane potential ($\Delta\Psi$) drops significantly (Zahrebelski et al., 1995). It is possible a similar sequence of events occurs in Clara cells treated with NA, but attempts to measure $\Delta\Psi$ or mitochondrial GSH levels have proven elusive, particularly as the required techniques are not well adapted to studying intact tissues and isolated Clara cells cannot satisfactorily be maintained in vitro. Using isolated airway explants, we observed a drastic reduction in ATP levels during brief in vitro exposures to NA metabolites (>70% loss in 30 minutes), not observed in DEM treated airways. NA itself did not significantly lower ATP levels in explants during but may have required a longer incubation period to generate reactive species via P450 metabolism of NA (Warren et al., 1982). This does not

explicity demonstrate that mitochondrial disruption is key to NA cytotoxicity nor does it implicate GSH loss in diminished ATP production. However, the in vitro assessment of ATP loss allowed us to provide a biochemical measure of function, which correlates with the pathological changes we observed in the mitochondria of Clara cells in vivo. The doses of NA, NA metabolites, and DEM used in the in vitro incubations in this study, are known to significantly deplete GSH within airway explants in vitro (Chichester et al., 1994; Duan et al., 1996). Naphthoquinones are known to deplete GSH and ATP and open the mitochondrial permeability transition pore in hepatocyte mitochondria (Gant et al., 1988; Henry and Wallace, 1996), while DEM does not deplete mitochondrial GSH pools in hepatocytes (Meredith and Reed, 1982). Therefore, the mitochondrial lesions caused by NA in vivo and ATP loss caused by NA metabolites in vitro, may be related to differing toxicities observed for NA and DEM in vivo, and may be related to the abilities of these compounds to affect mitochondrial GSH levels. Before this issue could be properly addressed, however, methods need to be developed to study mitochondrial function and/or measure mitochondrial GSH levels within pulmonary tissue as Clara cells cannot be maintained in culture, where most current methods are typically applied.

This study determined that a dramatic loss of GSH is by itself not a toxic event for Clara cells. We evaluated patterns of cytotoxicity and GSH loss, created by two distinctly different compounds (NA and DEM). Our results show that severe GSH loss in Clara cells causes substantial swelling, actin cytoskeleton disruptions, and plasma membrane blebbing. These types of cellular changes have been reported in cells exposed to various toxicants, and may represent a generic response of the cell to GSH loss and/or oxidative stress seen in the earliest stages of cell death (Jewell et al., 1982; Reed and Fariss, 1984; Mirabelli et al., 1988; Zahrebelski et al., 1995;

Manygoats et al., 2002). Necrotic cell death was only observed in Clara cells exposed to NA, where GSH loss and protein adduct formation are known to occur (Buckpitt et al., 2002). Our results clearly distinguish the different outcomes of these two treatments, but they could not isolate the specific cause of cell death in NA treated animals. Several possibilities exist to explain why DEM treated Clara cells do not become necrotic: 1) GSH protects cells from insult, so GSH depletion in the absence of a further insult (e.g. no protein adducts) is not lethal, 2) there are differences in the ability of the two treatments to deplete the mitochondrial GSH pool, assuming this pool is critical to mitochondrial function, and/or 3) covalent naphthalene protein adducts disrupt critical cellular functions that, in combination with glutathione depletion, lead to necrosis. Recent studies showing that several of the proteins adducted by reactive naphthalene metabolites are involved in protein folding, including calreticulin (Wheelock et al., submitted), protein disulfide isomerase and several heat-shock proteins ((Lin et al., 2005); Isbell et al., submitted), raised the possibility that glutathione depletion, and subsequent loss of a primary protective mechanism for the control of reactive oxygen species with decrements in the ability to repair damaged proteins leads to necrosis. Studies are currently underway to determine whether this hypothesis is tenable. Determining which of these possibilities is most relevant now that the response to GSH loss is defined, is the next step in determining the exact mechanism of toxicity for bioactivated toxicants such as NA.

Acknowledgements

Advice, technical assistance, and critical review provided by Dexter Morin and Dr. Alan Buckpitt was tremendously helpful. The assessment of pathology in electron micrographs provided by Dr. Dennis Wilson was greatly appreciated. Critical reading of the manuscript by Dr. Suzette Smiley-Jewell was very helpful.

References

Bereiter-Hahn J and Voth M (1994) Dynamics of mitochondria in living cells: shape changes, dislocations, fusion, and fission of mitochondria. *Microscopic Research Techniques* **27**:198-219.

Boyland E and Chasseaud LF (1967) Enzyme-catalysed conjugations of glutathione with unsaturated compounds. *Biochem J* **104**:95-102.

Buckpitt A, Boland B, Isbell M, Morin D, Shultz M, Baldwin R, Chan K, Karlsson A, Lin C, Taff A, West J, Fanucchi M, Van Winkle L and Plopper C (2002) Naphthalene-induced respiratory tract toxicity: metabolic mechanisms of toxicity. *Drug Metab Rev* **34**:791-820.

Buckpitt AR, Bahnson LS and Franklin RB (1984) Hepatic and pulmonary microsomal metabolism of naphthalene to glutathione adducts: factors affecting the relative rates of conjugate formation. *J Pharmacol Exp Ther* **231**:291-300.

Chevez-Barrios P, Wiseman AL, Rojas E, Ou CN and Lieberman MW (2000) Cataract development in gamma-glutamyl transpeptidase-deficient mice. *Exp Eye Res* **71**:575-582.

Chichester CH, Buckpitt AR, Chang A and Plopper CG (1994) Metabolism and cytotoxicity of naphthalene and its metabolites in isolated murine Clara cells. *Mol Pharmacol* **45**:664-672.

Deneke SM, Lynch BA and Fanburg BL (1985) Transient depletion of lung glutathione by diethylmaleate enhances oxygen toxicity. *J Appl Physiol* **58**:571-574.

Duan X, Plopper C, Brennan P and Buckpitt A (1996) Rates of glutathione synthesis in lung subcompartments of mice and monkeys: possible role in species and site selective injury. *J Pharmacol Exp Ther* **277**:1402-1409.

Dumont M, D'Hont C, Durand-Schneider AM, Legrand-Defretin VL, Feldmann G and Erlinger S (1991) Inhibition by colchicine of biliary secretion of diethylmaleate in the rat: evidence for microtubule-dependent vesicular transport. *Hepatology* **14**:10-15.

Ecobichon DJ (1984) Glutathione depletion and resynthesis in laboratory animals. *Drug Chem Toxicol* **7**:345-355.

Gant TW, Rao DN, Mason RP and Cohen GM (1988) Redox cycling and sulphydryl arylation; their relative importance in the mechanism of quinone cytotoxicity to isolated hepatocytes. *Chem Biol Interact* **65**:157-173.

Gerard-Monnier D, Fougeat S and Chaudiere J (1992) Glutathione and cysteine depletion in rats and mice following acute intoxication with diethylmaleate. *Biochem Pharmacol* **43**:451-456.

Henry TR and Wallace KB (1996) Differential mechanisms of cell killing by redox cycling and arylating quinones. *Arch Toxicol* **70**:482-489.

Jewell SA, Bellomo G, Thor H, Orrenius S and Smith M (1982) Bleb formation in hepatocytes during drug metabolism is caused by disturbances in thiol and calcium ion homeostasis. *Science* **217**:1257-1259.

Lakritz J, Plopper CG and Buckpitt AR (1997) Validated high-performance liquid chromatography-electrochemical method for determination of glutathione and glutathione disulfide in small tissue samples. *Anal Biochem* **247**:63-68.

Lin CY, Isbell AM, Morin D, Boland BC, Salemi MR, Jewell WT, Weir AJ, Fanucchi MV, Baker GL, Plopper CG and Buckpitt AR (2005) Characterization of a structurally intact in situ lung model and comparison of naphthalene protein adducts generated in this model vs. lung microsomes. *Chem Res Toxicol* **in press**.

Lowry OH, Rosebrough NJ, Lewis Farr A and Randall RJ (1951) Protein measurement with the folin phenol reagent. *J.Biol.Chem.* **193**:265-275.

Manygoats KR, Yazzie M and Stearns DM (2002) Ultrastructural damage in chromium picolinate-treated cells: a TEM study. Transmission electron microscopy. *J Biol Inorg Chem* **7**:791-798.

Martensson J, Jain A, Frayer W and Meister A (1989) Glutathione metabolism in the lung: inhibition of its synthesis leads to lamellar body and mitochondrial defects. *Proc Natl Acad Sci U S A* **86**:5296-5300.

Martensson J, Jain A, Stole E, Frayer W, Auld PA and Meister A (1991) Inhibition of glutathione synthesis in the newborn rat: a model for endogenously produced oxidative stress. *Proc Natl Acad Sci U S A* **88**:9360-9364.

Meredith MJ and Reed DJ (1982) Status of the mitochondrial pool of glutathione in the isolated hepatocyte. *J Biol Chem* **257**:3747-3753.

Mirabelli F, Salis A, Marinoni V, Finardi G, Bellomo G, Thor H and Orrenius S (1988) Menadione-induced bleb formation in hepatocytes is associated with the oxidation of thiol groups in actin. *Arch Biochem Biophys* **264**:261-269.

Nagelkerke JF, van de Water B, Twiss IM, Zoetewey JP, de Bont HJ, Dogterom P and Mulder GJ (1991) Role of microtubuli in secretion of very-low-density lipoprotein in isolated rat hepatocytes: early effects of thiol reagents. *Hepatology* **14**:1259-1268.

Phimister AJ, Lee MG, Morin D, Buckpitt AR and Plopper CG (2004) Glutathione Depletion Is a Major Determinant of Inhaled Naphthalene Respiratory Toxicity and Naphthalene Metabolism in Mice. *Toxicol Sci*.

Plopper C, Hyde D and Buckpitt A (1997) Clara Cells, in *The Lung: Scientific Foundations* (Crystal RG and West JB eds) pp 517-533, Raven Publishers, Philadelphia.

Plopper CG, Chang AM, Pang A and Buckpitt AR (1991) Use of microdissected airways to define metabolism and cytotoxicity in murine bronchiolar epithelium. *Exp Lung Res* **17**:197-212.

Plopper CG, Van Winkle LS, Fanucchi MV, Malburg SR, Nishio SJ, Chang A and Buckpitt AR (2001) Early events in naphthalene-induced acute Clara cell toxicity. II. Comparison of glutathione depletion and histopathology by airway location. *Am J Respir Cell Mol Biol* **24**:272-281.

Plummer JL, Smith BR, Sies H and Bend JR (1981) Chemical depletion of glutathione in vivo. *Methods Enzymol* **77**:50-59.

Reed DJ and Fariss MW (1984) Glutathione depletion and susceptibility. *Pharmacol Rev* **36**:25S-33S.

Sies H (1999) Glutathione and its role in cellular functions. *Free Radic Biol Med* **27**:916-921.

Uhlig S and Wendel A (1992) The physiological consequences of glutathione variations. *Life Sci* **51**:1083-1094.

Van Winkle LS, Buckpitt AR, Nishio SJ, Isaac JM and Plopper CG (1995) Cellular response in naphthalene-induced Clara cell injury and bronchiolar epithelial repair in mice. *Am J Physiol* **269**:L800-818.

Van Winkle LS, Johnson ZA, Nishio SJ, Brown CD and Plopper CG (1999) Early events in naphthalene-induced acute Clara cell toxicity: comparison of membrane permeability and ultrastructure. *Am J Respir Cell Mol Biol* **21**:44-53.

Warren DL, Brown DL, Jr. and Buckpitt AR (1982) Evidence for cytochrome P-450 mediated metabolism in the bronchiolar damage by naphthalene. *Chem Biol Interact* **40**:287-303.

West JA, Pakehham G, Morin D, Fleschner CA, Buckpitt AR and Plopper CG (2001) Inhaled naphthalene causes dose dependent Clara cell cytotoxicity in mice but not in rats. *Toxicol Appl Pharmacol* **173**:114-119.

Yagi H and Jerina D (1975) A General Synthetic Method for Non-K-Region Arene Oxides. *Journal of the American Chemical Society* **97**:3185-3191.

Zahrebelski G, Nieminen AL, al-Ghoul K, Qian T, Herman B and Lemasters JJ (1995) Progression of subcellular changes during chemical hypoxia to cultured rat hepatocytes: a laser scanning confocal microscopic study. *Hepatology* **21**:1361-1372.

Footnotes

Financial support provided by: National Institute of Environmental Health Sciences (R01 ES012720, R01 ES04311, R01 ES06700, R01 ES04699 and T32 ES07059) and State of California Tobacco Related Disease Research Program (11RT-0258). UC Davis is a National Institute of Environmental Health Sciences Center (P30 ES05707).

Portions of this research were presented previously: Phimister, A., Plopper, C. Role of glutathione depletion in toxicant induced injury to Clara cells. *Tox Sci.* (2003) 72 (S-1): 351

Address all correspondence to: Dr. Andrew J. Phimister, Department of Molecular Biosciences, University of California, Davis, CA 95616

Figure Legends

Fig. 1: Schematic of the differences between naphthalene (NA) and diethylmaleate (DEM) in regards to glutathione (GSH) depletion and possible mechanism(s) of cytotoxicity. Metabolism of NA by cytochrome P450 monooxygenase enzymes is obligate for toxicity and produces reactive metabolites (NAM; e.g. epoxides and naphthoquinones), which can form covalent protein adducts, react with GSH in solution, or be conjugated to GSH by glutathione-S-transferase enzymes (GSTs).(Buckpitt et al., 2002) In contrast, DEM requires active GSTs to deplete GSH.(Boyland and Chasseaud, 1967)

Fig. 2: GSH levels were measured directly by HPLC with electrochemical detection in homogenates of distal conducting airway segments isolated by microdissection from mice that were treated with NA (■) or DEM (■). Control time point represents mice 3 hours after treatment with corn oil (carrier). Data are the mean + S.E.M. n = 5 animals. *Significantly different from control $p< 0.05$.

Fig. 3: Ethidium homodimer-1 labeling was used as an indicator of cell necrosis (red dots) in the terminal airways of mice treated with NA or DEM. Cells were not permeable to ethidium homodimer-1 in vehicle control (3A) or DEM treated animals (3C) at any time point up to 24 hours after treatment (6 hour animals shown). Numerous permeable cells were present in the airways of NA treated animals 6 hours after treatment (3B, arrows; inset shows individual permeable cells in more detail). The cortical actin cytoskeleton (3D-F) of airway epithelial cells was imaged after labeling with direct-binding F-actin probe, Alexa 568 phalloidin. Ciliated cells (CC) and Clara cells (non-ciliated; NC) could be distinguished based on their appearance in

controls (3D). Treatment with either NA (3E) or DEM (3F) caused disruptions (asterisks) in the normal architecture of the actin cytoskeleton (compare with 3D). Airway epithelium (AE); parenchyma (PA). Magnifications: A-C, bar = 0.5 mm; C inset, bar = 20 μm; D-F, bar = 10 μm.

Fig. 4: Histopathologic assessment of terminal conducting airway epithelium from mice exposed to DEM, NA, or carrier (corn oil). Epithelium in carrier treated mice (4A) was of regular thickness and consisted of ciliated cells (CC) and non-ciliated cells (NC; i.e. Clara cells). Exposure to NA for 3, 6 or 24 hours (4B-4D respectively) caused Clara cells to become vacuolated (V) and to form massive apical membrane blebs (*). Frank necrotic cells were eventually exfoliated into the airway lumen. Squamated (i.e. flattened) ciliated cells covered the areas where Clara cells had exfoliated (arrows). Treatment with DEM for 3, 6, or 24 hours (4E-4G respectively) resulted in cellular swelling. Interstitial edema (arrowheads) was evident 24 hours after treatment with either NA or DEM (4D and 4G). 1-micron thick epoxy sections stained with toluidine blue. Representative micrographs. Bar = 10 μm.

Fig. 5: Ultrastructure of terminal bronchiolar epithelium in corn oil (carrier), NA, and DEM treated mice. The epithelium consists of mixture of ciliated (CC) and non-ciliated cells (NC; i.e. Clara cells). A prominent feature of murine Clara cells is the large apical protrusion extending into the airway lumen (5A). Higher magnification of the apical portion of the cell (5B) shows that Clara cells contain abundant secretory granules (G), smooth endoplasmic reticulum (SER), and mitochondria (M) in circular and longitudinal profile at the apex of the cell. Nuclei (Nu), Golgi bodies, and rough endoplasmic reticulum are typically confined to the basal portion of the Clara cell. Clara cells in mice exposed to NA (5C-E) underwent drastic changes in cell structure,

starting with swelling and cytoplasmic vacuole formation as early as 1 hour after treatment (5C). Cellular degeneration proceeded rapidly in NA treated tissues; with massive membrane blebs (asterisk) forming at the apices of affected Clara cells 3 hours after treatment (5D). These blebs were separated from the cytoplasm by thick bands of filaments (5D, space between arrows) and contained what appeared to be vacuolated and partially coalesced SER. The remaining cytoplasm was filled with swollen mitochondria. Degeneration resulted in necrotic Clara cells exfoliating (ExNC) into the lumen of the airways and squamated ciliated cells (SqCC) covering the basement membrane by 24 hours after treatment. No changes were noted 1 hour after DEM treatment, but by 3 hours Clara cells were swollen (5F) and had apical membrane blebs (5G, asterisk). Membrane blebs were separated from the cytoplasm by thick bands of filaments (5G, space between arrows) and contained mostly SER. Multilamellar bodies were often found within membrane blebs of DEM treated Clara cells (5G, arrowheads). Twenty-four hours after DEM treatment, swelling had largely resolved in Clara cells (5H), however, small membrane blebs (asterisk) were noted in some ciliated cells. Magnifications: A,C-H, bar = 5 μm; B, bar = 0.5 μm.

Fig. 6: Individual organelles were examined at higher magnification (12,500-40,000X) to investigate the effects of NA and DEM treatments on Clara cells. Mitochondria (M) in control cells were electron dense and contained few cristae (6A). Mitochondria in NA treated animals progressively lost electron density and became swollen (6B; 3 hour animal), appearing to disintegrate into fragments filled with dense spots between opaque areas by 6 hours (6C). Mitochondria in DEM treated Clara cells remained normal in appearance 3 hours after treatment (6D), but by 24 hours many had atypical branched morphologies and their cristae were more clearly apparent (6E-F). Clara cells are secretory cells and normally have prominent Golgi bodies

(GB; 6G). In DEM treated animals, the cisternae of the Golgi bodies were greatly distended with pericanalicular vesicles accumulating on the trans-side of the bodies 3 hours after treatment (6H). The Golgi body distension resolved by 24 hours (6I). In Clara cells exposed to NA, Golgi bodies could not easily be identified. Bars = 500 nm.

Fig. 7: Plot of ATP levels as measured in homogenates made from distal conducting airways isolated from untreated mice and incubated with toxicants *in vitro*. A luciferase-based methodology was used to measure ATP content. Airways were incubated with 0.35 mM DEM, 0.5 mM NA, 0.2 mM naphthalene-oxide (NA-oxide), 0.2 mM 2-methyl-1,4-naphthoquinone (MQ), or an equivalent volume of methanol (vehicle control). Methanol volume equaled 0.5% of the incubation volume. Data are the mean + S.E.M. $n \geq 5$ airways. * Significantly decreased relative to control $p < 0.05$.

Table 1: Pathology grading scores (mean ± S.E.M.)

	NA	DEM
control	0.1 ± 0.1	0.1 ± 0.1
3hr	3.0 ± 0.1	1.3 ± 0.2
6hr	3.4 ± 0.2	0.4 ± 0.1
24hr	4.0 ± 0.0	0.2 ± 0.1

JPET Fast Forward. Published on April 21, 2005 as DOI: 10.1124/jpet.105.084533

Figure 1

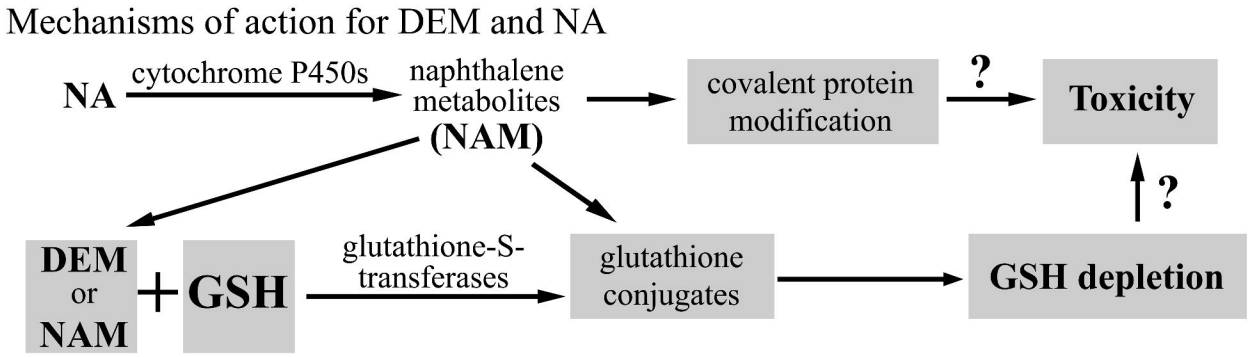

JPET Fast Forward. Published on April 21, 2005 as DOI: 10.1124/jpet.105.084533
This article has not been copyedited and formatted. The final version may differ from this version.

figure 2

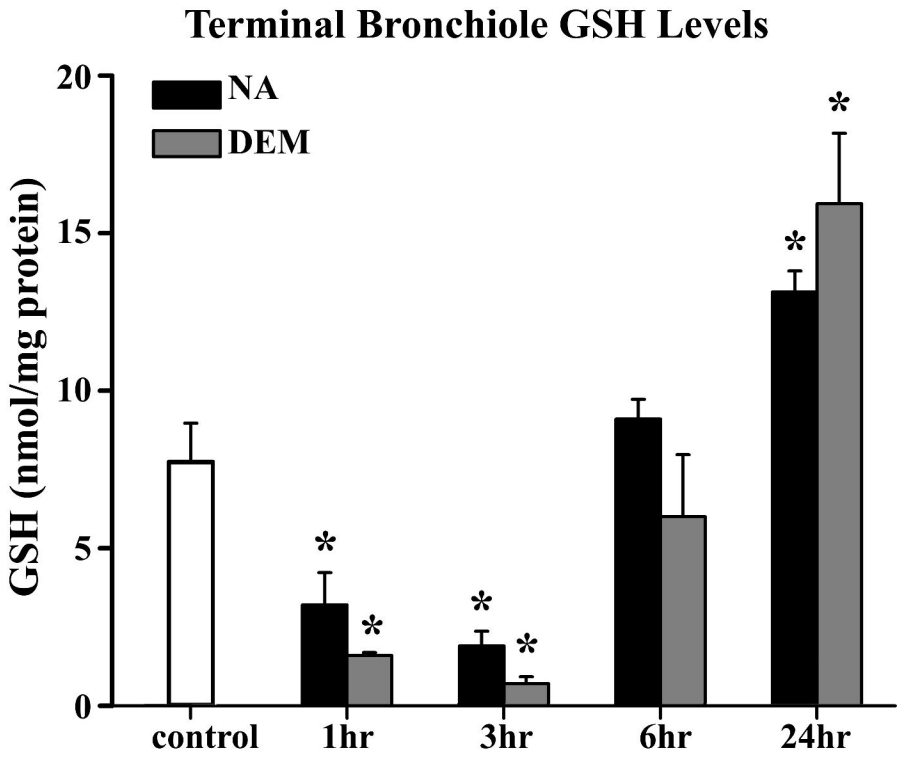

JPET Fast Forward. Published on April 21, 2005 as DOI: 10.1124/jpet.105.084533
This article has not been copyedited and formatted. The final version may differ from this version.

figure 3

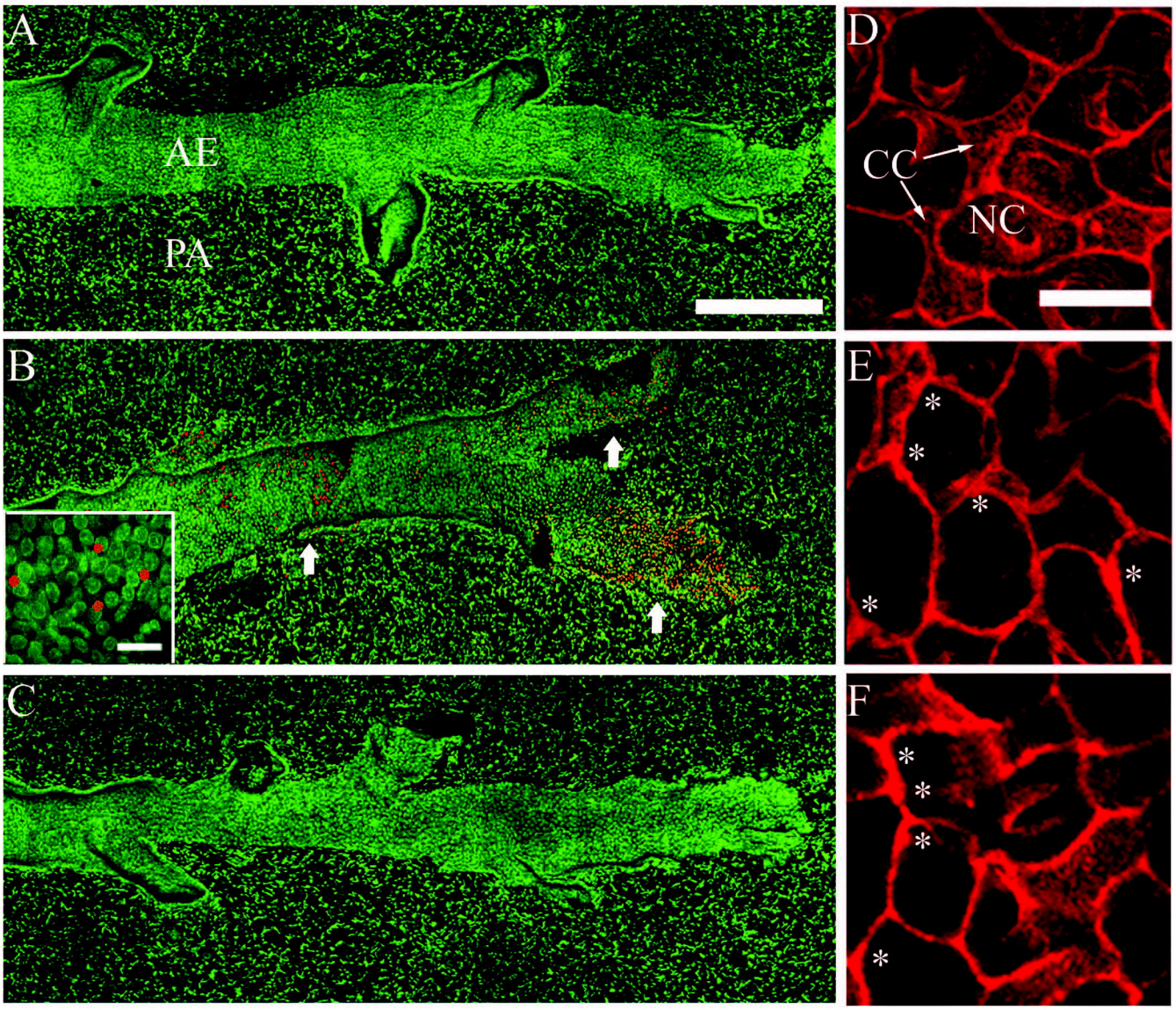

JPET Fast Forward. Published on April 21, 2005 as DOI: 10.1124/jpet.105.084533
This article has not been copyedited and formatted. The final version may differ from this version.

figure 4

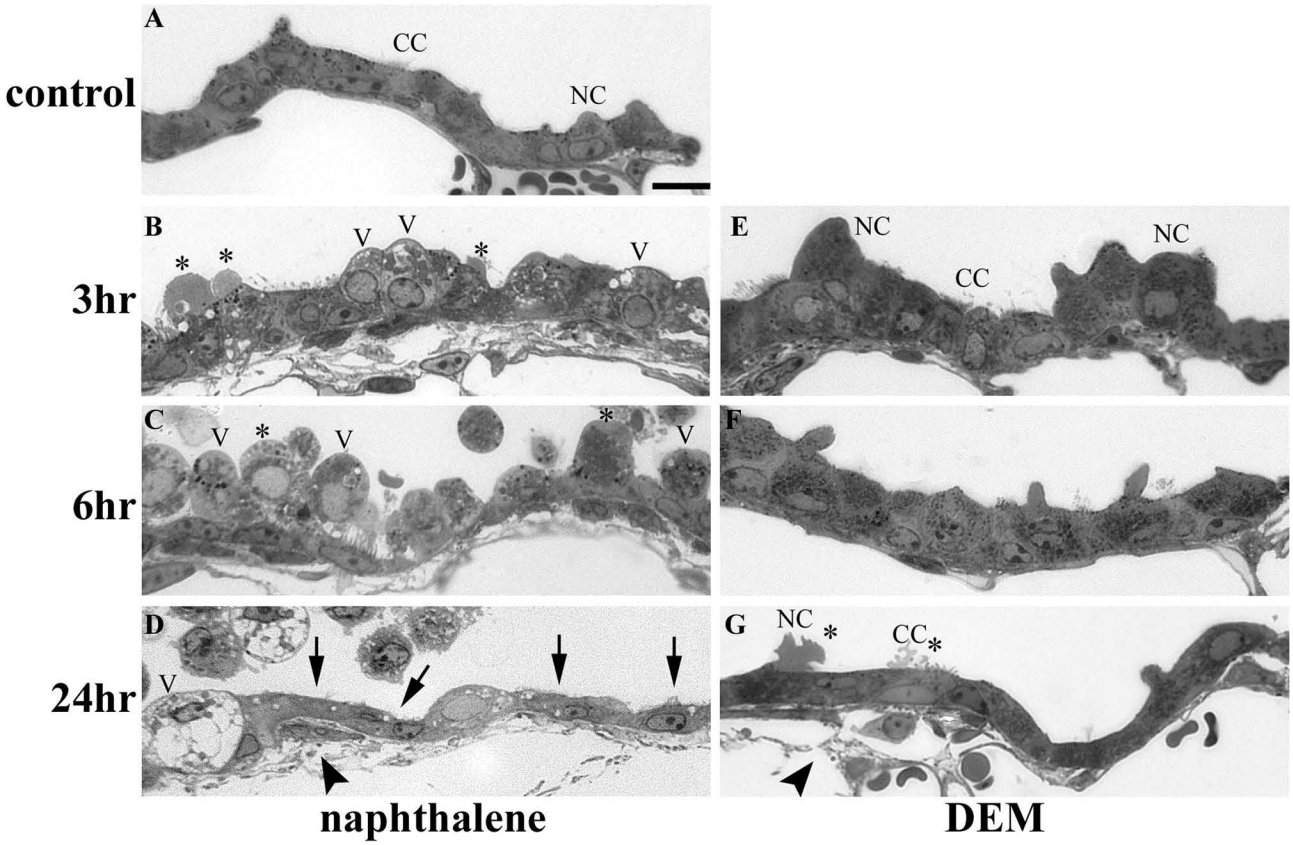

JPET Fast Forward. Published on April 21, 2005 as DOI: 10.1124/jpet.105.084533
This article has not been copyedited and formatted. The final version may differ from this version.

figure 5

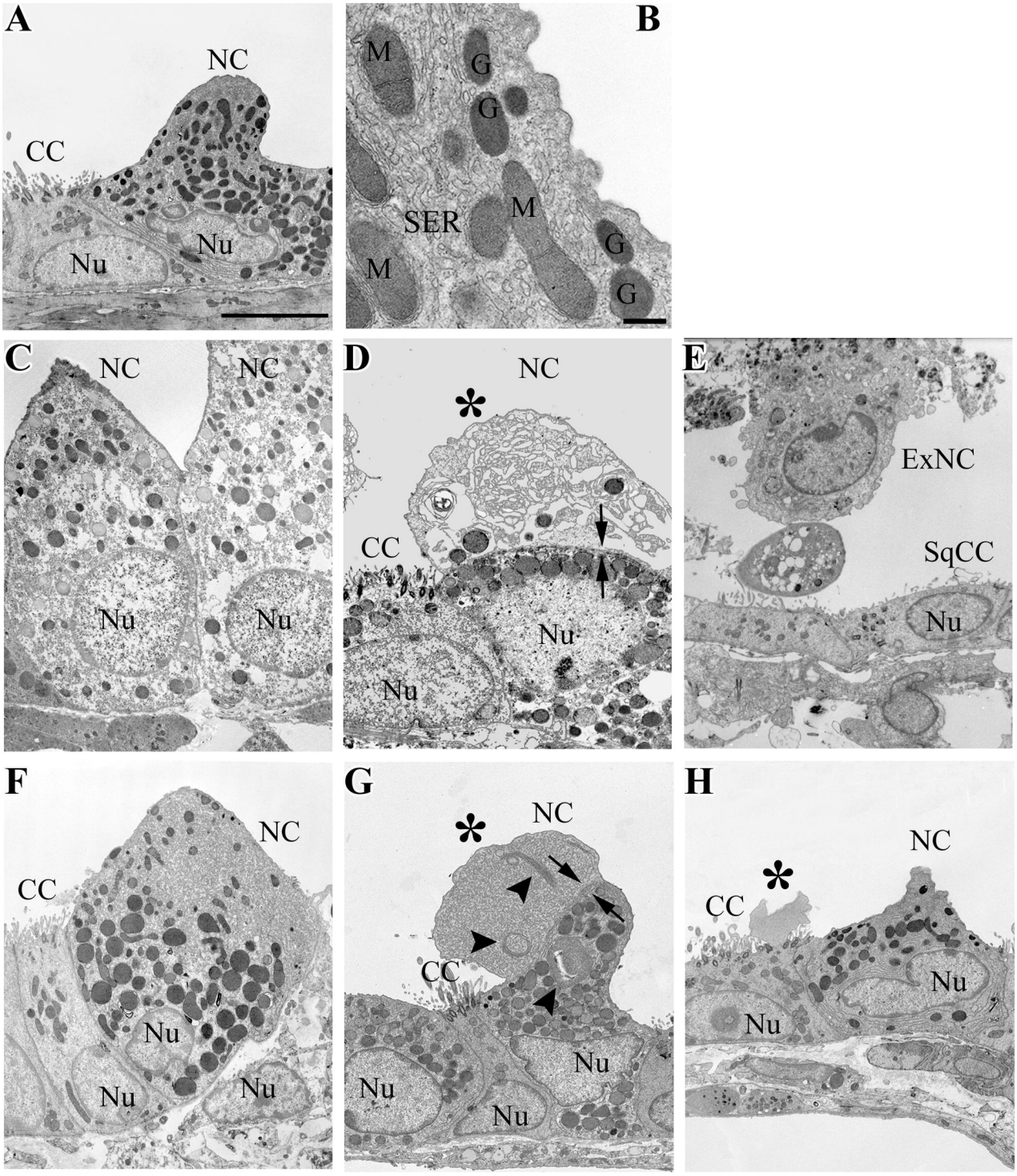

JPET Fast Forward. Published on April 21, 2005 as DOI: 10.1124/jpet.105.084533
This article has not been copyedited and formatted. The final version may differ from this version.

figure 6

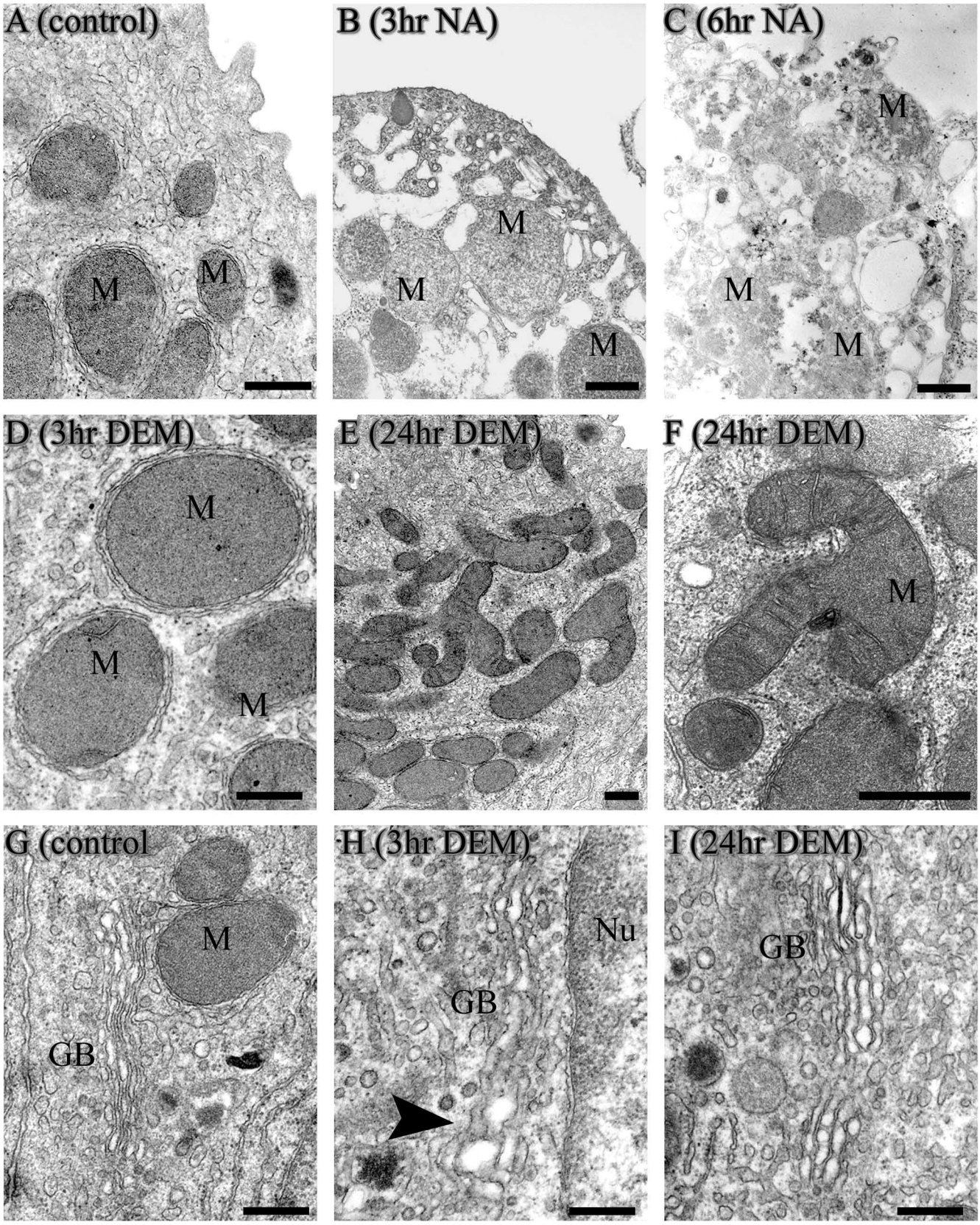

JPET Fast Forward. Published on April 21, 2005 as DOI: 10.1124/jpet.105.084533
This article has not been copyedited and formatted. The final version may differ from this version.

figure 7